Talanta 125 (2014) 418–424

Contents lists available at ScienceDirect

Talanta

journal homepage: www.elsevier.com/locate/talanta

"Turn-on" fluorescent dipodal chemosensor for nano-molar detection of Zn^{2+}: Application in living cells imaging

Umesh Fegade [a,c], Hemant Sharma [b], Banashree Bondhopadhyay [d], Anupam Basu [d], Sanjay Attarde [c], Narinder Singh [b,*], Anil Kuwar [a,**]

[a] School of Chemical Sciences, North Maharashtra University, Jalgaon 425001, Maharashtra, India
[b] Department of Chemistry, Indian Institute of Tecnhology, Ropar, Rupanagar, Punjab, India
[c] School of Environmental and Earth Sciences, North Maharashtra University, Jalgaon 425001, Maharashtra, India
[d] Molecular Biology and Human Genetics Laboratory, Department of Zoology, The University of Burdwan, Burdwan 713104, West Bengal, India

ARTICLE INFO

Article history:
Received 20 January 2014
Received in revised form
4 March 2014
Accepted 5 March 2014
Available online 13 March 2014

Keywords:
Zinc recognition
Fluorescence spectroscopy
Density functional theory
Live cell imaging

ABSTRACT

A malonohydrazide derivative bearing an imine and phenolic group was synthesized and had a high affinity and selectivity towards Zn^{2+}. The recognition properties of receptor **1** were evaluated using absorbance and fluorescence spectroscopy. The 1:1 stoichiometry of **1**.Zn^{2+} was confirmed from job's plot, mass spectra and density functional theory (DFT). The detection of Zn^{2+} in intracellular environment of HeLa cell through confocal microscopy was successfully applied for live cell imaging.

1. Introduction

In recent years, fluorophores gained a considerable space in the field of supramolecular chemistry due to score of applications like sensing and detection of transition metal ions, cell imaging, environmental and clinical roles [1–6]. Among transition metal ions, Zn^{2+} is the second most-abundant metal ion in our body and led several biological functions like influencing DNA synthesis, gene expression, enzyme catalysis, apoptosis, immune system function and neuronal signal transmission [7]. A disturbance in level of Zn^{2+} in our body cause several diseases like amyotrophic lateral sclerosis, epilepsy, Alzheimer's disease, loss of taste and hypoxia ischemia [8]. To date, several attempts have been made for the detection of Zn^{2+}; due to its electronic configuration ($3d^{10}$ $4s^0$) only possible technique to detect Zn^{2+} in biological system is fluorescence spectroscopy [9]. Generally, available probes sense the analyte through an increase or decrease of the emission intensity [10]. However, the emission intensity is also dependent on other factors, such as the sensor concentration, bleaching, optical path length, and illumination intensity [11]. It is therefore desirable to eliminate the effects of these factors by using a ratiometric sensor that exhibits a spectral shift upon binding to the analyte of interest, so that the ratio between the two emission intensities can be used to evaluate the analyte concentration [12–19].

Here we are paying attention for the development of ratiometric fluorescent sensor that utilized photo-induced electron-transfer (PET) and intramolecular charge-transfer (ICT) effect. The combination of PET and ICT produced the visual change for the detection of Zn^{2+} because PET produced enhancement or quenching in the intensity and ICT give shift in the absorption and emission wavelength. Generally these types of molecule are used as an anion sensor due to the presence of amine and hydroxyl group [17]. However, we are reporting PET and ICT based ratiometric fluorescent sensor **1** for the detection of Zn^{2+}. Coordination sites in the receptor **1** show that there are two amine groups and imine linkages with hydroxyl groups (Scheme 1). The binding ability of receptor **1** with various cations such as Cr^{3+}, Mn^{2+}, Fe^{3+}, Co^{2+}, Ni^{2+}, Cu^{2+}, Zn^{2+}, Cd^{2+}, Hg^{2+}, Pb^{2+} and Bi^{3+} was evaluated in DMSO/H_2O (50:50, v/v); computed the binding constant for **1**.Zn^{2+} and optimized its geometry through using Gaussian09 program.

2. Experimental detail

2.1. Reagents and apparatus

All commercial grade chemicals and solvents were purchased from Sigma-Aldrich Chemicals Ltd and used without further purification. ^1H and ^{13}C-NMR spectra were recorded on a Varian

* Corresponding author.
** Corresponding author. Tel.: +91 257 2257 432; fax: +91 257 2257 403.
E-mail address: kuwaras@gmail.com (A. Kuwar).

http://dx.doi.org/10.1016/j.talanta.2014.03.002
0039-9140/

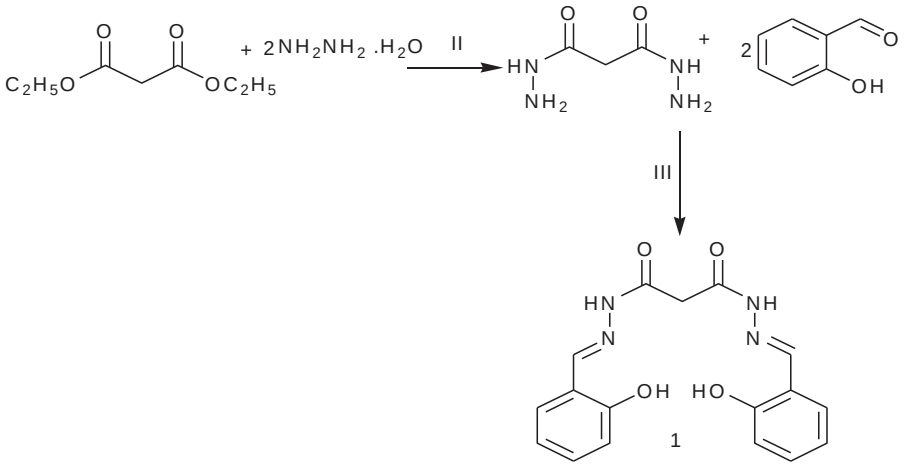

Scheme 1. Synthetic route of receptor **1** [(II) without solvent, stirring at room temperature, 0.5 h; (III) refluxing 1.5 h in ethanol].

NMR mercury System 300 spectrometer operating at 300 and 75 MHz in DMSO-*d6*. The fluorescence spectra were recorded on Fluoromax-4 spectrofluorometer and UV–visible spectra on Shimadzu UV–24500 UV–visible spectrophotometer at room temperature using 1 cm cell. The whole set of experiments were performed using DMSO/H_2O (50:50, v/v) solution as solvent system. In order to eliminate any error due to temperature and kinetic of reaction, all spectra were recorded after 15 min of solution preparation. Cell imaging experiment was done by Leica DM 1000 fluorescence microscope equipped with a UV filter.

2.2. Sample preparation

A stock solution of probe **1** (7 mM) was prepared in DMSO/H_2O (50:50, v/v) solution (receptor **1** is freely soluble in DMSO at 25 °C), and the corresponding working solutions (70 μM) were simply prepared by diluting with DMSO/H_2O (50:50, v/v) solution. All stock and working solutions were prepared in ultrapure water and spectroscopic grade DMSO. Stock solutions of all cations (70 mM) were prepared in DMSO/H_2O (50:50, v/v) solution and the corresponding working solutions (0.7 mM) were prepared by diluting with DMSO/H_2O (50:50, v/v).

2.3. UV visible analysis

The cation binding assay was performed on UV–visible spectrophotometer using 11 different metal ions (Cr^{3+}, Mn^{2+}, Fe^{3+}, Co^{2+}, Ni^{2+}, Cu^{2+}, Zn^{2+}, Cd^{2+}, Hg^{2+}, Pb^{2+} and Bi^{3+}) with receptor **1** in DMSO/H_2O (50:50, v/v) solvent system at room temperatures (298 K). For detail study, titrations were performed between receptor **1** and particular metal ion. It is also helpful for showing linear relationship between concentrations and the absorbance intensity; for calculating correlation coefficient. These titration experiments were accomplished through a stepwise addition of metal salt solutions (0.7 mM) to a solution of receptor **1** (70 μM) in DMSO/H_2O (50:50 v/v) in 10 ml volumetric flask. The absorbance intensity was recorded in the range of 200–600 nm alongside a reagent blank.

2.4. Fluorescence analysis

Similarly, metal binding test was carried out on Fluoromax-4 spectrofluorometer in DMSO/H_2O (50:50 v/v) solvent system at room temperatures (298 K). The titration was performed by successive addition of metal salt solutions (0.7 mM) to a solution of receptor **1** (70 μM) in DMSO/H_2O (50:50 v/v) in 10 ml volumetric flask. The association constant (K_a) and limit of detection was calculated from titration, which is performed between receptor **1** and Zn^{2+} in DMSO/H_2O (50:50 v/v) solvent system.

Using the Benesi–Hildebrand plot (Eq. (1)), Scatchard plot (Eq. (2)) and Connor plot (Eq. (3)) methodologies binding constant (K) was calculated.

$$1/F-F_0 = 1/(F_\infty - F_0)K[G]+1/(F_\infty - F_0) \quad (1)$$

$$F-F_0/[G] = (F_\infty - F_0)K-(F-F_0)K \quad (2)$$

$$1-F/F_0/[F] = K(F/F_0)-\alpha K \quad (3)$$

The stoichiometry between Zn^{2+} and receptor **1** was confirmed through Job's plot. In this method, the total concentration of the receptor **1** and metal ion was kept constant, with a continuous variable molar fraction of guest i.e. $[G]/([H]+[G])$. The maxima in the plot between $[HG]$ and $[H]/[H]+[G]$ correspond to stoichiometry of the complex. The fluorescence intensity was recorded at $\lambda_{ex}/\lambda_{em}$=320/470 nm alongside a reagent blank. The excitation and emission slits were both set to 5.0 nm. Each spectrum was recorded after 5 min interval (to ensure mixing).

2.5. In vitro cell imaging

Cellular imaging experiment was performed according to the method of Sen et al. [21] [20]. Human cervical cancer cell-HeLa cells, obtained from NCCS, Pune were grown in Dulbecco's Modified Eagle Medium (DMEM) supplemented with 10% Fetal Bovine Serum (FBS), 1% L-glutamine–penicillin–streptomycin and maintained at 37 °C in a humidified atmosphere with 5% CO_2. The cells after reaching 80–90% confluence were trypsinized (with 0.25% trypsin-EDTA) and seeded on the cover slip in the 35 mm culture dish with seeding density of 4×10^4 cells per 35 mm dish. After the cells have reached 60% confluence the media was replaced with fresh serum free media and 2 μM of receptor **1** was added. At the end of 30 min incubation with receptor **1**, Zn^{2+} (25 μM) were added to the culture medium and incubated for another 30 min at 37 °C for cellular uptake of Zn^{2+}. The cells were washed twice with 1× Phosphate Buffer Saline (PBS). The cover slip on which the cells were seeded was mounted on a glass slide and observed under fluorescence microscope (Leica DM 1000) with excitation at 320 nm.

2.6. Synthesis of receptor **1**

Receptor **1** was synthesized by reaction of one mole of diethyl malonate (0.32 g, 0.2 mmol) with two moles of hydrazine hydrate (0.20 g, 0.4 mmol) without solvent and stir for 30 min. Further, it was reacted with *O*-hydroxy benzaldehyde (0.49 g, 0. 4 mmol) in ethanol (50 ml) with refluxing for 1.5 h. Receptor **1** was obtained with quantitative yield and appearance of white powder. Yield-88%, Solubility in DMSO, mp-198–200 °C. ^{1}H-NMR (300 MHz, DMSO-d_6, ppm) δ=3.9 (s, 2*H*, CH_2), 6.5–7.0 (m, 6*H*, Ar–H), 7.798.1 (m, 4*H*, Ar–H), 11.4 (s, 2*H*, NH), 13.2 (s, 2*H*, Ar–OH). ^{13}C NMR, (75 MHz, DMSO-d_6, ppm) δ=40.5, 116.5, 118.6, 120.0, 131.3, 133.7, 159.0, 163.25 IR (KBr, cm^{-1}) υ=598, 750, 778, 894, 893, 1101, 1307, 1610, 1652, 3049, 3205. MS (ESI): *m*/*z* requires $C_{17}H_{16}N_4O_4$: 340.117, found 340.89.

2.7. Synthesis of Zn^{2+} complexes of receptor **1**

Zn^{2+} complex of receptor **1** was synthesized by reaction of one mole of receptor **1** (0.68 g, 0.2 mmol) with one moles of $ZnCl_2 \cdot 7H_2O$ (0.52 g, 0.2 mmol) in DMSO:MeOH (10:90, v/v, 50 ml). The mixture was allowed to stir for 3 h at room temperature and after some time solid product was separated out. The precipitate was collected by filtration at room temperature and dried in vacuum. Further, it was washed with water then ethanol followed by petroleum ether. Yield-84%, IR (KBr, cm^{-1}) υ=682, 750, 783, 893, 1197, 1379, 1572, 1620, 2923. MS (ESI): *m*/*z* requires $C_{17}H_{14}N_4O_4Zn$: 403.71, found 404.83

3. Result and discussion

3.1. Synthesis of receptor **1**

Receptor **1** was synthesized by reaction of diethyl malonate with hydrazine hydrate to obtain malonohydrazide and further it was reacted with salicyladehyde in ethanol with stirring for 1.5 h (Scheme 1). The receptor **1** was obtained with quantitative yield and having white appearance. The synthesized receptor was characterized by various techniques such as melting point, IR, ^{1}H-NMR, ^{13}C-NMR and mass spectroscopic methods. The spectral investigation gave consistent data of structure of receptors **1**.

3.2. UV–visible studies of receptor **1**

The absorption behaviour of receptor **1** (70 μM) upon interacting with various transition metal ions was studied in DMSO/H_2O (50:50 v/v) solvent system. The absorption spectra of receptor **1** contain three maxima at 281, 291 and 320 nm as shown in Fig. 1A. It is observed that with the addition of Zn^{2+} a new band is appeared at 373 nm and simultaneously band at 320 nm is disappeared (Fig. 1A). This shift in the wavelength is due to the ligand to metal charge transfer and it appears that the core functionality required for **1** to efficiently bind Zn^{2+}. For in depth study, a titration is performed between receptor **1** with Zn^{2+} ion. The successive addition of Zn^{2+} produce a ratiometric response having two isosbestic points at 310 and 340 nm as shown in Fig. 1B. This indicates that the existence of one equilibrium in the system. To confirm the relationship between ratiometric intensity and concentration of Zn^{2+}; graph is plotted among normalized fluorescence intensity vs log [Zn^{2+}] (Fig. 1B inset). The linear dependence of concentration of Zn^{2+} authenticate that receptor **1** could be utilized for quantitative determination of Zn^{2+} ion.

3.3. Fluorescence studies of receptor **1**

Like absorption spectroscopy, metal binding test is also performed on emission spectroscopy using the similar conditions. A series of 11 transition metals are added separately along with receptor **1** (70 μM) in 5 ml volumetric flasks in DMSO/H_2O (50:50, v/v) solvent system as shown in Fig. 2. Most of metal ions did not show any change in emission profile of receptor **1** expect Zn^{2+} (Fig. 2). The addition of Zn^{2+} (0.7 mM) resulted in a remarkably enhancement of fluorescence intensity along with small red shift in λ_{max} (Δ=10 nm). Beside that it also showed visual change from colourless to blue green fluorescent colour under UV light as shown in inset of Fig. 2.

Further, titration was carried out to confirm the mechanism of binding. The gradual addition of Zn^{2+} leads to enhancement and red shift in fluorescence intensity as shown in Fig. 3. The inset represents the linear relationship between normalized fluorescence intensity and log [Zn^{2+}] at 470 nm. The addition of one equivalent of Zn^{2+} led to significant enhancement and slight red shift (Δ=10 nm) in fluorescence intensity of receptor **1**. Further addition of Zn^{2+} did not produce any change in the emission profile. It infers that Zn^{2+} and receptor **1** form complex in 1:1

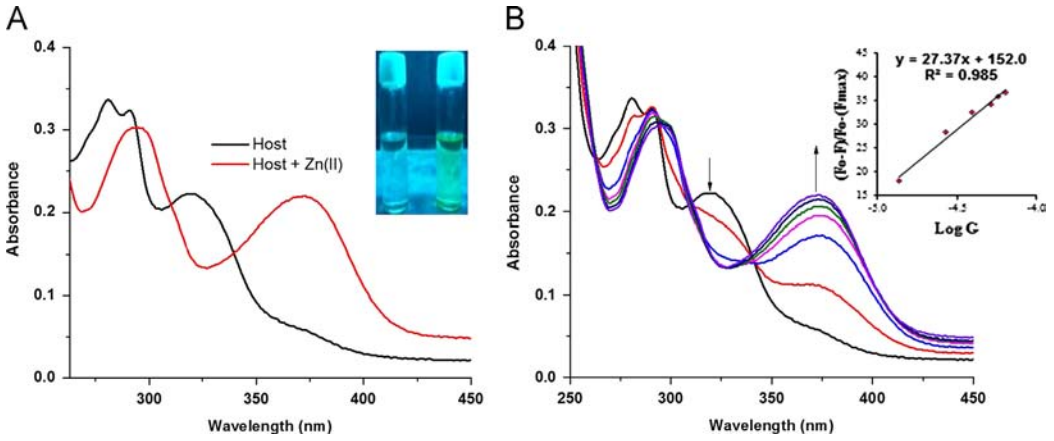

Fig. 1. (A) Changes in absorbance spectrum of receptor **1** (70 μM) upon the addition of Zn^{2+} metal ion (0.7 mM) in DMSO/H_2O (50:50, v/v) solvent system (inset represent the visual change in the solution of receptor **1** upon addition of Zn^{2+} ion); (B) change in absorption profile of receptor **1** (70 μM) upon gradually addition of Zn^{2+} metal ion (0 to 0.7 mM) in DMSO/H_2O (50:50, v/v). The inset shows the linear dependence among normalized fluorescence intensity $(F_o-F)/F_o-(F_{max})$ and log [Zn^{2+}] with regression 0.985.

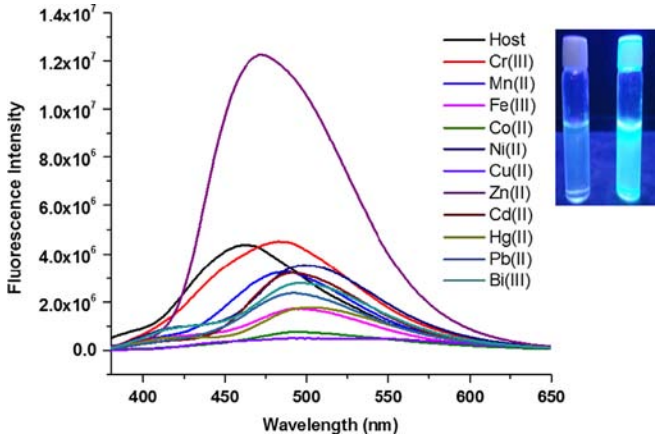

Fig. 2. Fluorescence spectra (λ_{ex}=320 nm) of receptor **1** (70 μM) upon the addition of fixed amount of metal salts (0.7 mM) in DMSO/H_2O (50:50, v/v) solvent system. The inset illustrates colour change upon addition of Zn^{2+} in DMSO: H_2O (50:50, v/v) solution under UV light (from left to right: **1** only, **1**.Zn^{2+}). (For interpretation of the references to color in this figure legend, the reader is referred to the web version of this article.)

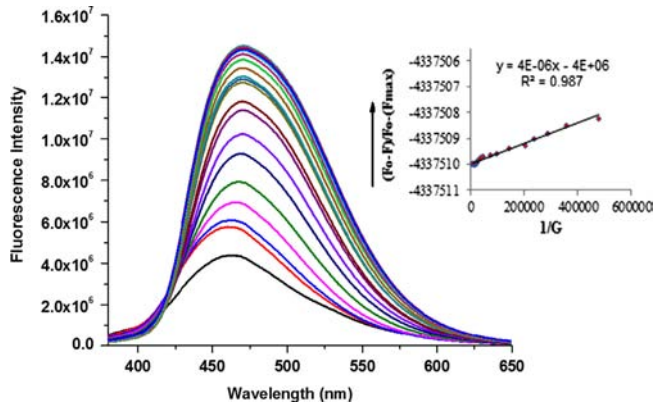

Fig. 3. Fluorescence titration of receptor **1** (70 μM) upon the addition of Zn^{2+} salt (0.7 mM) in DMSO/H_2O (50:50, v/v) solvent system; the inset represents that Normalized response of fluorescence signal with regression 0.987.

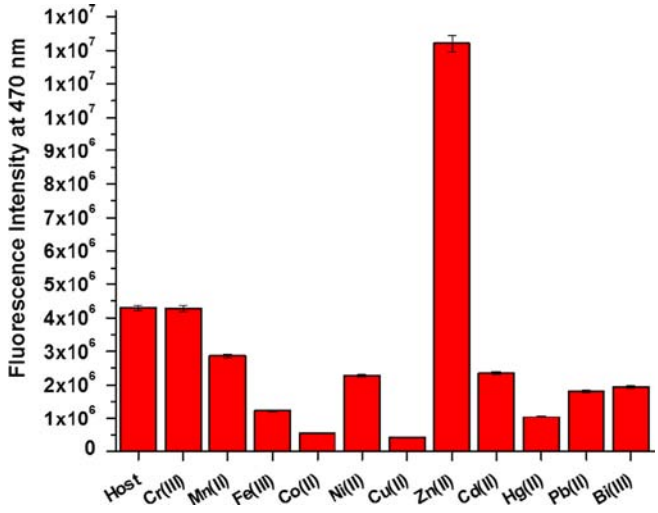

Fig. 4. Fluorescence intensity of receptor **1** (70 μM) upon the addition of a particular metal salt (0.7 mM) in DMSO/H_2O (50:50, v/v).

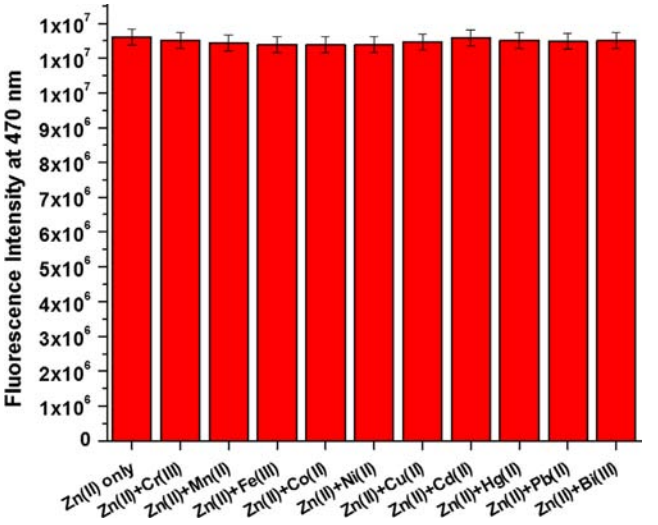

Fig. 5. A competitive binding assay of receptor **1** towards Zn^{2+} in the presence and absence of other metal ions.

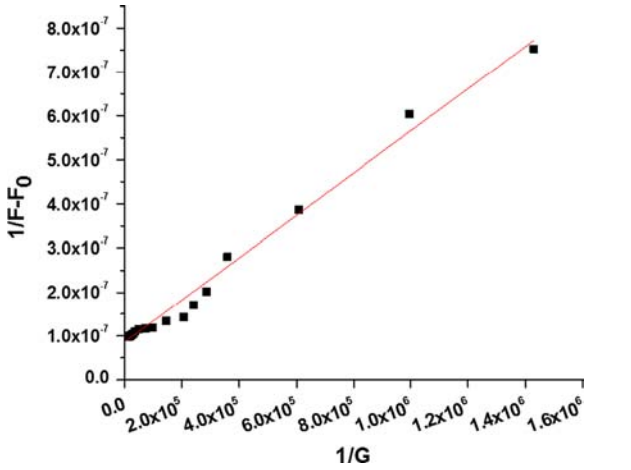

Fig. 6. Benesi–Hildebrand Plot receptor **1** (adjusted equation: $1/F-F_0=4.2\times10^{-13}+9.0\times10^{-8}1/[G]$, R=0.989) at the K_a value 214286 M^{-1}.

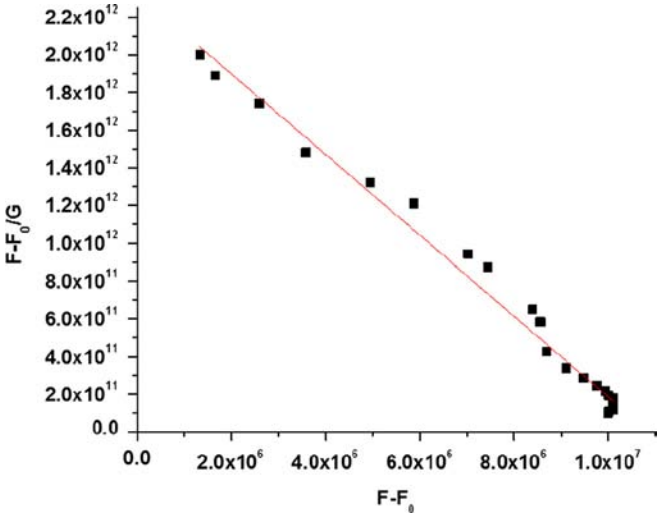

Fig. 7. Scatchard Plot receptor **1** (adjusted equation: $F-F_0/[G]=-213377+2.0\times10^{12}$, R=0.9872) at the K_a value 213377 M^{-1}.

stoichiometry, which is also supported from job's plot and mass spectra. As a consequence of coordination of Zn^{2+} with two oxygen of hydroxyl groups, electronic current of **1** was disturbed and cause enhancement with red shift. Therefore, PET and ICT are two possible processes behind this phenomenon [20]. Moreover, receptor **1** shows the importance of hydroxyl group participation in Zn^{2+} binding. The hydroxyl group is act as a good binding site and plays an effective role in binding of transition metal ions [21,22].

To examine the selectivity of receptor **1** towards Zn^{2+}, series of competitive titrations were performed in the presence and absence of other competing cations. A set of solutions were made having same equivalent of Zn^{2+} and different metal ion along with receptor **1**. The receptor **1** has high selectivity even in the presence of other competing cations as shown in Figs. 4 and 5. It still has excellent turn-on fluorescence response for the detection of Zn^{2+} and it confirmed the high selectivity of receptor **1** for Zn^{2+} shown in Figs. 4 and 5.

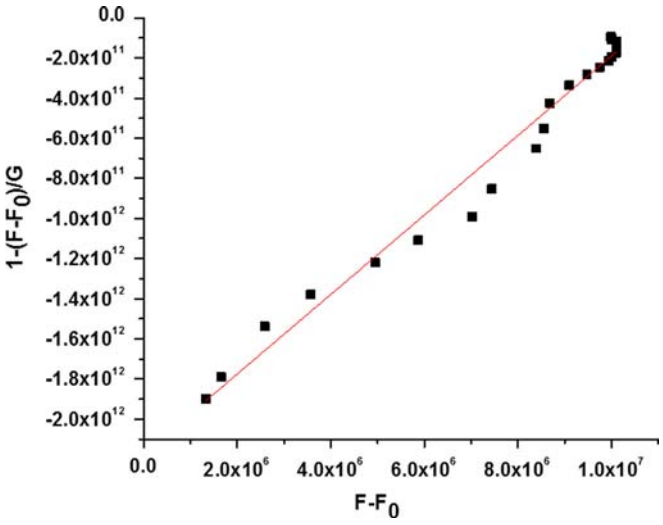

Fig. 8. Connor Plot receptor **1** (adjusted equation: $y=213377x-2.0\times10^{12}$, $R=0.987$) at the K_a value 213377 M^{-1}.

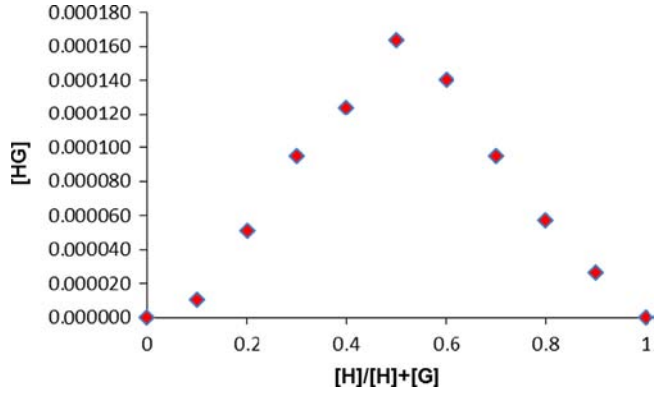

Fig. 9. A Job plot between **1** and Zn^{2+} representing the stoichiometry of the host: guest (1:1).

3.4. Binding constant, detection limit and stoichiometry of receptor *1*

In order to determine the binding constant, Benesi–Hildebrand plot, Scatchard plot and Connor plot methodologies was used and K_a was about $(2.1\pm0.3)\times10^5\ M^{-1}$ (Figs. 6–8) [23–25]. The method of continuous variation (Job's plot) was employed to find the stoichiometry of complex **1**.Zn^{2+} [26]. The graph was plotted between [*HG*] and [*H*]/([*H*]+[*G*]) and has maxima at 0.5 which corresponds to 1:1 stoichiometry of complex **1**.Zn^{2+} (Fig. 9). Further, ESI-MS spectra were recorded and has peak at *m/z* 404.83, which corresponds to 1:1 stoichiometry of complex **1**.Zn^{2+} (Fig. S1). IR spectrum of the zinc complex indicated that hydroxyl groups of receptor **1** take part in the complexation with zinc because the band responsible for hydroxyl protons is absent in **1**.Zn^{2+} complex IR (Fig. S2 and S3). Under optimal conditions, the detection limit for Zn^{2+} was as low as 35 nM. Further, the quantum yields of receptor **1** and **1**.Zn^{2+} were calculated using literature method and it was about 0.28 and 0.64 [27].

Table 1
An optimized bond angles, dihedral angles and energy calculated at B3LYP/6-31G level.

Parameter	Receptor 1	1.Zn^{2+}
Dihedral angles (°)		
N6–N4–C1–C2	−175.68	−128.31
N7–N5–C3–C2	173.66	−178.49
N4–N6–C34–C16	173.99	157.04
N5–N7–C35–C26	−174.13	−157.28
Bond angles (°)		
N6–N4–C1	121.93	115.5
N7–N5–C3	122.29	115.06
C1–C2–C3	115.82	103.07
C34–N6–N4	122.5	124.91
C35–N7–N5	121.87	128.87
Bond length ()		
O36–Zn42	–	1.81
O37–Zn42	–	1.83
C3–O9	1.25	1.27
C1–O8	1.24	1.23
Energy (eV)	Keto 32026.09	80425.18
EHOMO–LUMO (eV)	Keto 3.152	3.039

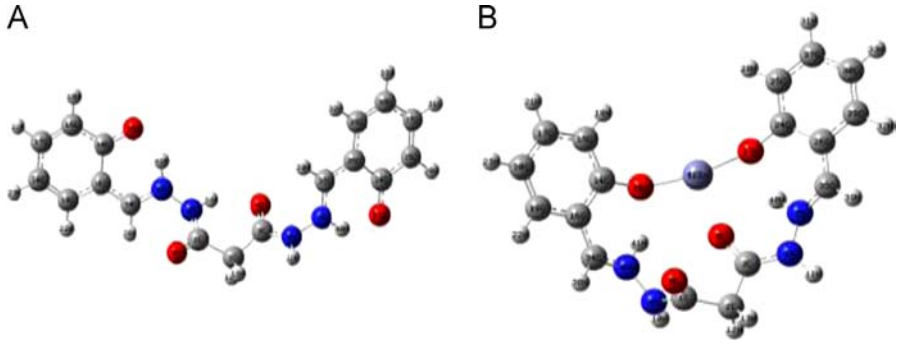

Fig. 10. The DFT optimized structure of: (A) Keto form of receptor 1, and (B) 1.Zn^{2+} calculated at the B3LYP/6-31G level. In which Zn is bind with the two hydroxyl oxygen after deportations.

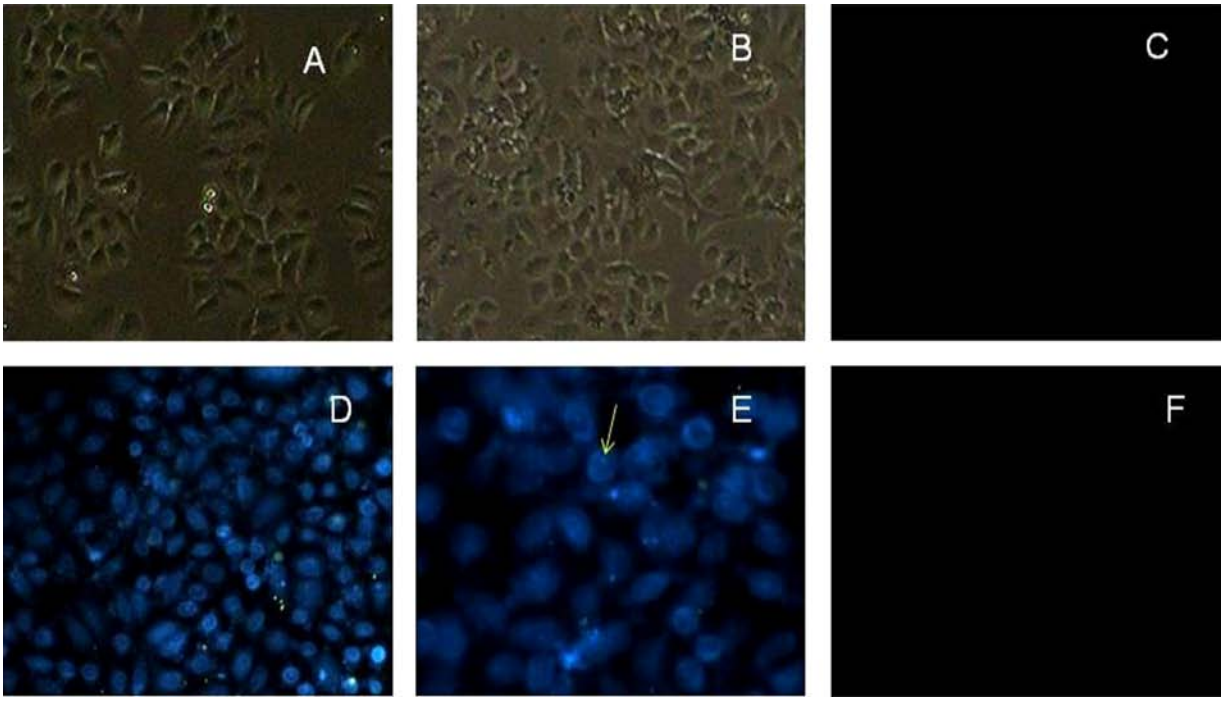

Fig. 11. Fluorescence images of HeLa cells with receptor **1** and Zn^{2+}. (A) Phase contrast image of control cells devoid of receptor **1** and Zn^{2+} (20 ×), (B) phase contrast image of HeLa cells challenged with receptor **1** (2 μM), (C) fluorescence photo-micrograph of cells incubated with only receptor **1**, (D) fluorescence photo-micrograph of cells incubated with receptor **1** and Zn^{2+} (20 ×), (E) in higher magnification (40 ×) of fluorescence photo-micrograph, nuclear uptake of Zn^{2+} is visible [arrow head]. (F) Fluorescence photo-micrograph of cells incubated with only Zn. (All fluorescence images were taken using excitation filter 320 nm).

3.5. *Colorimetrically naked eye detection*

The remarkable feature of this study is visual change upon addition of Zn^{2+}. This colorimetric and fluorescent response increased the scope of this methodology because it gives ON-SITE detection of Zn^{2+} in real environment. The inset of Fig. 1A and Fig. 2 illustrate the colorimetric and fluorescent colour change which can be visualized by the naked eye and under UV irradiation. The receptor **1** (70 μM) is colourless in DMSO/H_2O (50:50 v/v) solvent system and addition of 10 eq. of Zn^{2+} result into coloured solution.

3.6. *Proposed binding mode of **1** and **1**.Zn^{2+} from DFT calculation*

All optimization studies were carried out by using B3LYP/631G basis set on Gaussian 09 program [28–30]. The Keto form of receptor **1** has non-planar geometry in which two arms are totally opposite in direction (Fig. 10). However, it showed drastic change in geometry on addition Zn^{2+}, two arms come closer to each other and form an appropriate pseudocavity for Zn^{2+}. The various angles and dihedral angles are listed in Table 1 which represents the change in geometry on coordination with Zn^{2+}. A DFT optimized structure of complex **1**.Zn^{2+} is also explained fluorescent nature of complex. The Zn^{2+} has vacant d-orbital and it occupies the electron from coordinating oxygen atom which results into PET ON (Fig. 10) and theoptimized bond angles, dihedral angles and energy calculated at B3LYP/6-31G level is shown in Table 1.

4. Application of receptor 1

4.1. *Cellular imaging study*

Inspired from the above results like ON-SITE detection, visual color change and high selectivity for Zn^{2+}, receptor **1** was used for intracellular detection of Zn^{2+} in HeLa cell Line. To perform this study, HeLa cell was incubated in three different medium (a) enrich with receptor **1**, (b) Zn^{2+} only (c) both receptor **1** and Zn^{2+} respectively at 37 °C in a humidified atmosphere with 5% CO_2 [31]. It is observed that blue fluorescence was seen in case of those cells, which was incubated with both receptor **1** and Zn^{2+} as shown in Fig. 11D. However, no fluorescence was observed in other case as shown in Fig. 11.

5. Conclusion

In conclusion, we have designed and developed a selective and sensitive ratiometric fluorescent receptor **1** for the detection of Zn^{2+} in semi aqueous medium. The PET and ICT was possible mechanism behind this detection. The binding constant and detection limit revealed that receptor **1** has high selectivity towards Zn^{2+} and detect the Zn^{2+} upto 35 nM. Sensing in living cells have been developed by this probe for in vitro imaging. This new Zn^{2+} selective fluorescent probe could find potential biomedical applications.

Appendix A. Supporting information

Supplementary data associated with this article can be found in the online version at http://dx.doi.org/10.1016/j.talanta.2014.03.002.

References

[1] J.M. Lehn, Supramolecular Chemistry-Concept and Perspective, VCH, Weinheim, 1995.
[2] G. Wei, J. Yina, X. Ma, S. Yu, D. Wei, Y. Dua, Anal. Chim. Acta 703 (2011) 219–225.
[3] P.A. Kumar, V.T. Ramakrishnan, P. Ramamurthy, J. Phys. Chem. A 115 (2011) 14292–14299.
[4] N. Basaric, N. Doslicc, J. Ivkovic, Y.H. Wang, J. Veljkovic, K.M. Majerski, P Wan, J. Org. Chem. 78 (2013) 1811–1823.

[5] H. Sharma, N. Kaur, T. Pandiyan, N. Singh, Sens. Actuators, B 472 (2012) 166–167.
[6] A. Kaur, H. Sharma, S. Kaur, N. Singh, N. Kaur, RSC Adv. 3 (2013) 6160–6166.
[7] S.J. Lippard, J.M. Berg, Principles of Bioinorganic Chemistry, University Science Books, Mill Valley, CA, 1994.
[8] S.Y. Assaf, S.H. Chung, Nature 308 (1984) 734–736.
[9] R.Y. Tsien, in: A.W. Czarnik (Ed.), Fluorescent and Photochemical Probes of Dynamic Biochemical Signals inside Living Cells, American Chemical Society, Washington, DC, 1993, pp. 130–146.
[10] S.H. Lee, S.H. Kim, S.K. Kim, J.H. Jung, J.S. Kim, J. Org. Chem. 70 (2005) 1463–1466.
[11] Y.D. Fernandez, A.P. Gramatges, V. Amendola, F. Foti, C. Mangano, P. Pallavicini, S. Patroni, Chem. Commun. 14 (2004) 1650–1651.
[12] H. Chen, Y. Wu, Y. Cheng, H. Yang, F. Li, P. Yang, C. Huang, Inorg. Chem. Commun. 10 (2007) 1413–1415.
[13] Y.J. Zheng, J. Orbulescu, X.J. Ji, F.M. Andreopoulos, S.M. Pham, R.M. Leblanc, J. Am. Chem. Soc. 125 (2003) 2680–2686.
[14] K. Hiratani, M. Albrecht, Chem. Soc. Rev. 37 (2008) 2413–2421.
[15] H. Sharma, N. Kaur, N. Singh, Inorg. Chim. Acta 391 (2012) 83–87.
[16] U. Fegade, S. Attarde, A. Kuwar, Chem. Phys. Lett. 584 (2013) 165–171.
[17] U. Fegade, H. Sharma, K. Tayade, S. Attarde, N. Singh, A. Kuwar, Org. Biomol. Chem. 11 (2013) 6824–6828.
[18] U. Fegade, H. Sharma, K. Tayade, S. Attarde, N. Singh, A. Kuwar, Urea Based Dipodal, J. Fluorescence 24 (2014) 27–37.
[19] U. Fegade, J. Marek, R. Patil, S. Attarde, A. Kuwar, J. Lumin. 146 (2014) 234–238.
[20] G. Zhang, H. Li, S. Bi, L. Song, Y. Lu, L. Zhang, J. Yu, L. Wang, Analyst 138 (2013) 6163–6170.
[21] S. Sen, S. Sarkar, B. Chattopadhyay, A. Moirangthem, A. Basu, K. Dhara, P. Chattopadhyay, Analyst 137 (2012) 3335–3342.
[22] U. Fegade, A. Singh, G.K. Chaitanya, N. Singh, S. Attarde, A. Kuwar, Spectrochim. Acta, Part A 121 (2014) 569–574.
[23] H.A. Benesi, J.H. Hildebrand, J. Am. Chem. Soc. 71 (1949) 2703–2707.
[24] G. Scatchard, Ann. N.Y. Acad. Sci. 51 (1949) 660–672.
[25] K.A. Connors, Binding Constants: The Measurements of Molecular Complex Stability, Wiley, New York, 1987.
[26] P. Job, Ann. Chim. 9 (1928) 113–203.
[27] A.T.R. Williams, S.A. Winfield, J.N. Miller, Analyst 108 (1983) 1067–1070.
[28] A.D. Becke, J. Chem. Phys. 98 (1993) 5648–5652.
[29] C. Lee, W. Yang, R.G. Parr, Phys. Rev. B: Condens. Matter 37 (1988) 785–789.
[30] N. Singh, N. Kaur, R.C. Mulrooney, J.F. Callan, Tetrahedron Lett. 49 (2008) 6690–6692.
[31] W. Bruening, P. Moffett, S. Chia, G. Heinrich, J. Pelletier, FEBS Lett. 393 (1996) 41–47.